

The 191 Orientable Octahedral Manifolds

Damian Heard, Ekaterina Pervova, and Carlo Petronio

CONTENTS

- 1. Introduction
- 2. Preliminaries
- 3. Hyperbolic Manifolds
- 4. Nonhyperbolic Manifolds
- Acknowledgments
- References

We enumerate all the spaces obtained by gluing in pairs the faces of the octahedron in an orientation-reversing fashion. Whenever such a gluing gives rise to nonmanifold points, we remove small open neighborhoods of these points, so we actually deal with three-dimensional manifolds with (possibly empty) boundary.

There are 298 combinatorially inequivalent gluing patterns, and we show that they define 191 distinct manifolds, of which 132 are hyperbolic and 59 are not. All the 132 hyperbolic manifolds have already been considered in different contexts by other authors, and we provide here their known “names” together with their main invariants. We also give the connected sum and JSJ decompositions for the 59 nonhyperbolic examples.

Our arguments make use of tools coming from hyperbolic geometry, together with quantum invariants and more classical techniques based on essential surfaces. Many (but not all) proofs were carried out by computer.

1. INTRODUCTION

At the very beginning of his fundamental book [Thurston 79], as an example of the richness of topology in three dimensions, Bill Thurston mentioned the fact that there are quite a few inequivalent ways of gluing together in pairs the faces of the octahedron. However, to our knowledge, until now, nobody had ever exactly determined the number of nonhomeomorphic 3-manifolds arising as the results of these gluings. In this note we give a full solution to this problem, in the context of orientable (but unoriented) manifolds. After proving that there are 298 inequivalent gluing patterns, we have in fact proved the following:

Theorem 1.1. *Let O be the octahedron and let \mathcal{O} be the set of homeomorphism types of 3-manifolds that can be obtained as follows:*

- *First, glue together in pairs in a simplicial and orientation-reversing fashion the faces of O , thus getting a compact polyhedron X .*

2000 AMS Subject Classification: Primary 57M50; Secondary 57M25

Keywords: 3-manifolds, hyperbolic geometry, octahedron, JSJ decomposition

- *Second, remove from X disjoint open stars of the nonmanifold points, thus getting a compact orientable 3-manifold with (possibly empty) boundary, all the components of which have positive genus.*

Then \mathcal{O} contains precisely 191 elements, of which 132 are hyperbolic and 59 are not. More precisely, the numbers of inequivalent gluings and manifolds are split according to the topological type of the boundary as shown in Table 1, where Σ_g denotes the orientable surface of genus g .

For the PL notions of *polyhedron*, *manifold*, and *star*, see for instance [Rourke and Sanderson 72]. As usual [Benedetti and Petronio 92, Ratcliffe 06, Thurston 79], a 3-manifold M is *hyperbolic* if M minus the boundary components of M homeomorphic to the torus Σ_1 carries a complete metric with constant sectional curvatures -1 and totally geodesic boundary. The removed tori give rise to the so-called *cusps* of the manifold.

In addition to proving Theorem 1.1, we provide rather detailed information on the 191 elements of \mathcal{O} . In particular, we determine the volume and other invariants for the 132 hyperbolic manifolds in \mathcal{O} , and we identify the “names” they were given either in the Callahan–Hildebrand–Weeks census [Callahan et al. 99, Weeks 93] of small cusped hyperbolic manifolds, or in the Frigerio–Martelli–Petronio census [Frigerio et al. 04a, Frigerio et al. 04b] of small hyperbolic manifolds with geodesic boundary. We also give detailed descriptions for the 59 nonhyperbolic elements of \mathcal{O} . The list of the initial 298 inequivalent gluing patterns, and the triangulations (in SnapPea [Weeks 93] format) of the final 191 manifolds, together with geometric information for the hyperbolic ones, is available from [Heard et al. 08].

The question of counting the elements of \mathcal{O} has a rather transparent combinatorial flavor and appears to be well suited to computer investigation. The approach we have chosen relies on some rather sophisticated geometric tools developed over the last three decades by a number of mathematicians, and it has the additional advantage of providing detailed information on the final 191 manifolds, besides distinguishing them. To analyze the initial 298 manifolds, we have in fact employed the machinery of hyperbolic geometry and its algorithmic aspects (Thurston’s hyperbolicity equations [Thurston 79], the Epstein–Penner [Epstein and Penner 88] and Kojima [Kojima 90, Kojima 92] canonical decompositions, the Sakuma–Weeks [Sakuma and Weeks 95] and Ushijima [Ushijima 02] tilt formulas), and other powerful topological instruments (the prime [Hempel 76] and JSJ [Jac

and Shalen 78, Johannson 79] decompositions, the theory of normal surfaces [Haken 61], and the Turaev–Viro invariants [Turaev and Viro 92]).

We thank the referee for pointing out that the counting process, without the additional benefit of a detailed knowledge of the resulting manifolds, could have been carried out by computer almost completely using more classical tools, particularly the homology of finite covers. The fact that a majority of the manifolds we have found turn out to be hyperbolic can be viewed as a manifestation of the crucial role played by hyperbolic geometry in the context of three-dimensional topology, as chiefly witnessed by Thurston’s geometrization, now apparently proved by Perelman [Thurston 79, Perelman 02, Perelman 03a, Perelman 03b].

To prove Theorem 1.1, we have written some small specific Haskell code (available from [Heard et al. 08]) to list the combinatorially inequivalent gluing patterns, and then we have used the Orb and Manifold Recognizer programs [Heard 06, Matveev and Tarkaev 06] to match or distinguish the resulting manifolds. There were, however, some manifolds for which the computer was unable to find hyperbolic structures and some pairs of manifolds that it was unable to tell apart. In these instances, we had to work by hand using classical techniques, including properly embedded essential surfaces.

More to the point, to ensure that our final list of 191 manifolds is indeed correct, despite having been obtained by computer, we have adopted the following safeguards:

- We have obtained the list of the 298 inequivalent gluings of \mathcal{O} by running a single Haskell program after having carefully tested its various parts.
- We have then subdivided the 298 manifolds into classes according to their boundary, which of course we could do quickly and without risk of miscalculations.
- On each boundary class we have run two pieces of Orb code; the first one built (approximate) hyperbolic structures for many manifolds and grouped the manifolds according to volume and fundamental group (when it was able to recognize isomorphism); the second piece tried to match the triangulations within each set coming from the previous step; the result was the list of $17 + 30 + 7 + 79 + 2 + 56 = 191$ manifolds that eventually turned out to be the correct one; to show this our steps were as follows.
- We employed Orb to match all the manifolds indicated by it to be hyperbolic with the manifolds

Boundary Type	#(Gluing)	Hyperbolic	Nonhyperbolic	Total
\emptyset	37	–	17	17
Σ_1	81	9	21	30
$\Sigma_1 \sqcup \Sigma_1$	9	2	5	7
Σ_2	113	63	16	79
$\Sigma_2 \sqcup \Sigma_1$	2	2	–	2
Σ_3	56	56	–	56
Total	298	132	59	191

TABLE 1. Numbers of distinct manifolds arising from orientation-reversing gluings of the faces of an octahedron, with open stars of the nonmanifold points removed.

in the known hyperbolic censuses [Callahan et al. 99, Weeks 93] (for manifolds with torus boundary) and [Frigerio et al. 04a, Frigerio et al. 04b] (for manifolds with higher genus boundary); the fact that manifolds found by Orb to be distinct were also listed as distinct by these sources was useful in cross-checking that the program was behaving correctly.

- We were left to confirm that the manifolds not found by Orb to be hyperbolic were indeed not hyperbolic, and distinct unless matched by Orb. To do this we separated the class of manifolds with genus-2 boundary from the other ones:
 - Excluding the class with genus-2 boundary, we employed the Recognizer; the program was totally successful in detecting topological obstructions to hyperbolicity and in telling manifolds apart, with a single exception for a pair of closed manifolds that we had to distinguish by theoretical means (see below for details).
 - For the 16 genus-2 boundary items, we constructed by hand essential annuli—thus hyperbolicity was impossible in all cases—and then we analyzed the homology of finite covers, which left us with only two pairs of potentially equal but not matched manifolds; again we distinguished them theoretically, as explained below.

It is perhaps worth remarking that the three most problematic pairs just mentioned consist of distinct manifolds sharing the same fundamental group.

1.1 Issues of Numerical Accuracy

As already mentioned, the hyperbolic structures constructed by Orb [Heard 06] are found by numerical approximation only. In the cusped case they have been checked using exact arithmetic in algebraic number fields

with the program Snap [Goodman 03], by Oliver Goodman. For manifolds with geodesic boundary, our hyperbolic structures are indeed only approximate ones, but we have found complete agreement with the results in [Frigerio et al. 04a], where numerical approximation was also used, but the C++ code written to this end was totally independent of Orb. We also note that for some of the manifolds (in particular, for those with genus-3 boundary), hyperbolicity can also be established by theoretical means.

2. PRELIMINARIES

In this section we collect some elementary facts needed to prove Theorem 1.1.

2.1 Polyhedra versus Manifolds

Given a gluing pattern φ for the faces of the octahedron O , as described in the statement of Theorem 1.1, let us denote by $X(\varphi)$ the polyhedron resulting from the gluing, and by $M(\varphi)$ the 3-manifold obtained from $X(\varphi)$ by removing disjoint open stars of the nonmanifold points. The following easy fact, which we leave to the reader, shows that $X(\varphi)$ and $M(\varphi)$ are in fact very tightly linked:

Proposition 2.1.

- *Only the points of $X(\varphi)$ arising from the vertices of O can be nonmanifold points of $X(\varphi)$.*
- *The homeomorphism type of $X(\varphi)$ determines that of $M(\varphi)$, and conversely.*

Before proceeding, recall that \mathcal{O} denotes the set of homeomorphism classes of all $M(\varphi)$'s as φ varies in the set of simplicial and orientation-reversing gluing patterns of the faces of O .

2.2 Number of Inequivalent Gluings

To count the elements of \mathcal{O} , the first step is of course to enumerate the combinatorially inequivalent gluing patterns φ . Since O has eight faces and there are three different ways of gluing together any two chosen faces, the number of different patterns is $(8-1)!! \times 3^4 = 105 \times 81 = 8505$. However, there is a symmetry group with 48 elements acting on O , so the inequivalent patterns are actually much fewer than 8505. Using a small piece of Haskell code we have in fact shown the following:

Proposition 2.2. *There exist 298 combinatorially inequivalent patterns of orientation-reversing gluings of the faces of O .*

2.3 Classification According to Boundary Type

Two homeomorphic manifolds of course have homeomorphic boundaries. Moreover, the boundary of an orientable 3-manifold is an orientable surface, which is very easy to identify by counting the number of connected components and computing the Euler characteristic of each of them. So the first easy step toward understanding \mathcal{O} and proving Theorem 1.1 is to split the inequivalent gluing patterns according to the boundary they give rise to. Using again a Haskell program, we found the results described in the second column of Table 1.

2.4 Further Notation

Choosing one representative for each equivalence class of gluing patterns φ and constructing the corresponding manifold $M(\varphi)$, we get a set of 298 manifolds that we denote henceforth by \mathcal{M} . By definition, \mathcal{O} is obtained from \mathcal{M} by identifying homeomorphic manifolds, and the main issue in establishing Theorem 1.1 is indeed to determine which elements of \mathcal{M} are in fact homeomorphic to each other. Taking advantage of the easy work already described, we denote by \mathcal{M}_Σ the set of elements of \mathcal{M} having boundary Σ , thus getting a splitting of \mathcal{M} as

$$\mathcal{M} = \mathcal{M}_\emptyset \sqcup \mathcal{M}_{\Sigma_1} \sqcup \mathcal{M}_{\Sigma_1 \sqcup \Sigma_1} \sqcup \mathcal{M}_{\Sigma_2} \sqcup \mathcal{M}_{\Sigma_2 \sqcup \Sigma_1} \sqcup \mathcal{M}_{\Sigma_3}.$$

Each set \mathcal{M}_Σ , after identification of homeomorphic manifolds, gives rise to some \mathcal{O}_Σ , which we further split as

$$\mathcal{O}_\Sigma = \mathcal{O}_\Sigma^{\text{hyp}} \sqcup \mathcal{O}_\Sigma^{\text{non}},$$

separating the hyperbolic members from the non-hyperbolic ones.

3. HYPERBOLIC MANIFOLDS

According to the well-known *rigidity* theorem [Thurston 79, Benedetti and Petronio 92, Ratcliffe 06], each 3-manifold carries, up to isometry, at most one hyperbolic structure, as defined after the statement of Theorem 1.1. Note that the hyperbolic structures we consider are finite-volume by default. Moreover the following facts hold:

1. Every hyperbolic manifold with cusps or nonempty boundary has a “canonical decomposition,” which allows the efficient comparison of it to any other such manifold. This is the decomposition into ideal polyhedra due to Epstein and Penner [Epstein and Penner 88] for *cusped* manifolds (noncompact and without boundary), and the decomposition into truncated hyperideal polyhedra due to Kojima [Kojima 90, Kojima 92] for manifolds with nonempty boundary. The hyperbolic structure of a manifold, whence (by rigidity) its topology, determines not only the polyhedral type of the blocks of the decomposition, but also the combinatorics of the gluings.
2. If a manifold is represented by a *triangulation*, namely as a gluing of tetrahedra, both its hyperbolic structure (if any) and its canonical decomposition can be searched algorithmically. This applies in particular to any element of the set \mathcal{M} of manifolds we need to analyze, because the octahedron O can be viewed as a partial gluing of four tetrahedra. The idea to construct the hyperbolic structure, due to Thurston [Thurston 79], is to consider a space of parameters for the hyperbolic structures on each individual tetrahedron, and then to express the matching of the structures on the glued tetrahedra by a system of equations, which can be solved using numerical tools. The method for constructing the canonical decomposition is to modify any given geometric triangulation until the canonical decomposition is reached. This uses the “tilt formula” of Sakuma and Weeks [Sakuma and Weeks 95] for cusped manifolds, and its variation due to Ushijima [Ushijima 02], together with some ideas from [Frigerio and Petronio 04], for manifolds with nonempty geodesic boundary. Neither the search for the hyperbolic structure nor that for the canonical decomposition is fully guaranteed to work, but in practice they always do (perhaps after some initial randomization of the triangulation).
3. The computer programs SnapPea [Weeks 93], by Jeff Weeks, and Orb [Heard 06], by Damian Heard, very

efficiently implement the procedures mentioned in the previous point (even if SnapPea does not deal with manifolds with geodesic boundary); the same procedures were also used to produce the census [Frigerio et al. 04a] of hyperbolic manifolds with geodesic boundary up to complexity 4.

- Both SnapPea and Orb employ numerical approximation. Moreover, in the cusped case, the solutions found can be checked using exact arithmetic in algebraic number fields with the program Snap.

3.1 Genus-3 Geodesic Boundary

To prove Theorem 1.1, for each of the six sets \mathcal{M}_Σ that we have, we need to determine which elements of \mathcal{M}_Σ are homeomorphic to each other, thus finding the corresponding \mathcal{O}_Σ , and then to decide which elements of \mathcal{O}_Σ are actually hyperbolic. We begin with the case $\Sigma = \Sigma_3$, where the result is quite striking. It was initially discovered from a computer experiment [Frigerio et al. 04a] and later established theoretically. We include a sketch of the proof for the sake of completeness.

Proposition 3.1. *The 56 elements of \mathcal{M}_{Σ_3} are all hyperbolic and distinct from each other, so $\mathcal{O}_{\Sigma_3} = \mathcal{O}_{\Sigma_3}^{\text{hyp}} = \mathcal{M}_{\Sigma_3}$ has 56 elements. For each element of this set, the Kojima canonical decomposition has the same single block, namely a truncated regular hyperbolic octahedron with all dihedral angles equal to $\pi/6$.*

Proof: An easy computation of Euler characteristic shows that a gluing φ defines a manifold $M(\varphi)$ bounded by Σ_3 if and only if it identifies all 12 edges to each other. We want to show that such an $M(\varphi)$ is hyperbolic with geodesic boundary by choosing a hyperbolic shape of the truncated octahedron that is matched by φ . Since all edges are glued together, this can happen only if the geometric shape is such that all edges have the same length, i.e., the octahedron is regular. If this is the case, all dihedral angles are also the same, so they must all be $2\pi/12$. Such an octahedron certainly does not exist in Euclidean or spherical geometry, but it does in hyperbolic geometry. This implies that $M(\varphi)$ is indeed hyperbolic.

Let us now analyze the Kojima canonical decomposition of $M(\varphi)$. To this end we recall [Kojima 90, Kojima 92] that it is dual to the cut locus of the boundary, i.e., to the set of points having multiple shortest paths to $\partial M(\varphi)$. Using the fact that $M(\varphi)$ is the gluing of a regular truncated octahedron, which is totally symmetric, it is not too difficult to show that the Kojima decompo-

No.	Sym	Hom	No.	Sym	Hom
0	trivial	\mathbb{Z}^3	28	trivial	\mathbb{Z}^3
1	trivial	\mathbb{Z}^3	29	trivial	\mathbb{Z}^3
2	trivial	\mathbb{Z}^3	30	trivial	\mathbb{Z}^3
3	trivial	\mathbb{Z}^3	31	\mathbb{Z}_2	\mathbb{Z}^3
4	trivial	\mathbb{Z}^3	32	\mathbb{Z}_2	\mathbb{Z}^3
5	trivial	\mathbb{Z}^3	33	\mathbb{Z}_2	\mathbb{Z}^3
6	trivial	\mathbb{Z}^3	34	\mathbb{Z}_2	\mathbb{Z}^3
7	trivial	\mathbb{Z}^3	35	\mathbb{Z}_2	\mathbb{Z}^3
8	trivial	\mathbb{Z}^3	36	\mathbb{Z}_2	\mathbb{Z}^3
9	trivial	\mathbb{Z}^3	37	trivial	$\mathbb{Z}_3 + \mathbb{Z}^3$
10	trivial	\mathbb{Z}^3	38	\mathbb{Z}_2	$\mathbb{Z}_3 + \mathbb{Z}^3$
11	trivial	\mathbb{Z}^3	39	D_2	$\mathbb{Z}_3 + \mathbb{Z}^3$
12	D_2	\mathbb{Z}^3	40	\mathbb{Z}_4	$\mathbb{Z}_3 + \mathbb{Z}^3$
13	\mathbb{Z}_2	\mathbb{Z}^3	41	\mathbb{Z}_2	\mathbb{Z}^3
14	\mathbb{Z}_2	\mathbb{Z}^3	42	trivial	\mathbb{Z}^3
15	trivial	\mathbb{Z}^3	43	\mathbb{Z}_2	\mathbb{Z}^3
16	D_2	\mathbb{Z}^3	44	\mathbb{Z}_2	\mathbb{Z}^3
17	\mathbb{Z}_2	\mathbb{Z}^3	45	\mathbb{Z}_2	\mathbb{Z}^3
18	D_4	\mathbb{Z}^3	46	trivial	\mathbb{Z}^3
19	\mathbb{Z}_2	\mathbb{Z}^3	47	trivial	\mathbb{Z}^3
20	\mathbb{Z}_2	\mathbb{Z}^3	48	\mathbb{Z}_2	\mathbb{Z}^3
21	D_4	\mathbb{Z}^3	49	trivial	\mathbb{Z}^3
22	\mathbb{Z}_2	\mathbb{Z}^3	50	\mathbb{Z}_2	\mathbb{Z}^3
23	\mathbb{Z}_2	\mathbb{Z}^3	51	trivial	\mathbb{Z}^3
24	\mathbb{Z}_2	\mathbb{Z}^3	52	trivial	\mathbb{Z}^3
25	trivial	\mathbb{Z}^3	53	trivial	\mathbb{Z}^3
26	trivial	\mathbb{Z}^3	54	\mathbb{Z}_2	\mathbb{Z}^3
27	trivial	\mathbb{Z}^3	55	\mathbb{Z}_2	\mathbb{Z}^3

TABLE 2. Information on the 56 elements of $\mathcal{O}_{\Sigma_3}^{\text{hyp}}$ (the compact orientable hyperbolic manifolds with geodesic boundary of genus 3 arising from gluings of the octahedron). We note that all these manifolds have volume $11.448776110\dots$ and can be found in the file `census_4_T3_octa.snp` available from [Frigerio et al. 04b].

sition is given by the octahedron itself, with its gluing pattern φ . This implies that the geometry of $M(\varphi)$, and hence its topology, determines φ . Therefore different φ 's give rise to different $M(\varphi)$'s. □

It follows from this result that the 56 elements of $\mathcal{O}_{\Sigma_3}^{\text{hyp}}$ all have the same volume, which one can calculate to be $11.448776110\dots$ via Ushijima's formulas [Ushijima 06]. Using Orb, we have also computed the symmetry groups and homology of the elements of $\mathcal{O}_{\Sigma_3}^{\text{hyp}}$, as described in Table 2.

Note that these invariants alone are far from sufficient to distinguish the 56 elements of \mathcal{M}_{Σ_3} from one another. The table also shows the position of the manifolds in the file `census_4_T3_octa.snp` available from [Frigerio et al. 04b]. Here and below, \mathbb{Z}_n and D_n denote respectively

File	No.	Volume	Sym	Hom
census_4_cusp.snp	14	8.681737155	\mathbb{Z}_2	\mathbb{Z}^3
census_4_cusp.snp	15	8.681737155	\mathbb{Z}_2	\mathbb{Z}^3

TABLE 3. Information on the two elements of $\mathcal{O}_{\Sigma_2 \sqcup \Sigma_1}^{\text{hyp}}$ (the orientable hyperbolic manifolds with one cusp and geodesic boundary of genus 2 arising from gluings of the octahedron).

the cyclic group with n elements and the dihedral group with $2n$ elements.

3.2 Genus-2 Geodesic Boundary and One Cusp

For the case $\Sigma = \Sigma_2 \sqcup \Sigma_1$, the analysis of \mathcal{M}_Σ is already contained in [Frigerio et al. 04a]:

Proposition 3.2. *The two elements of $\mathcal{M}_{\Sigma_2 \sqcup \Sigma_1}$ are hyperbolic and distinct from each other, so $\mathcal{O}_{\Sigma_2 \sqcup \Sigma_1}^{\text{hyp}} = \mathcal{M}_{\Sigma_2 \sqcup \Sigma_1}$ has two elements.*

Table 3 describes the symmetry group and homology of both elements of $\mathcal{O}_{\Sigma_2 \sqcup \Sigma_1}^{\text{hyp}}$, and reference to their position in the files available from [Frigerio et al. 04b], as we determined using Orb.

3.3 Genus-2 Geodesic Boundary

The following partial information on the elements of \mathcal{M}_{Σ_2} can be deduced from the results in [Frigerio et al. 04a]:

Proposition 3.3. *The set \mathcal{M}_{Σ_2} (which has 113 elements) contains the following subsets:*

- A set of 14 distinct hyperbolic manifolds with Kojima decomposition having one and the same block, namely a regular truncated octahedron with all dihedral angles equal to $\pi/3$.
- A set of 8 distinct hyperbolic manifolds with Kojima decomposition having one and the same block, namely a nonregular truncated octahedron.
- A set of 4 distinct hyperbolic manifolds with Kojima decomposition having the same two blocks, namely two identical square pyramids.

Moreover, any other hyperbolic element of \mathcal{M}_{Σ_2} has Kojima decomposition consisting of tetrahedra only.

To complete the analysis of the hyperbolic elements of \mathcal{M}_{Σ_2} , we proved the following using Orb (and then matching the results to those in [Frigerio et al. 04a]):

Proposition 3.4. *Of the $113 - (14 + 8 + 4) = 87$ elements of \mathcal{M}_{Σ_2} not covered by Proposition 3.3, at least 37 are hyperbolic, and they are all distinct from one another.*

After Orb has been able to construct the hyperbolic structure of an element M of \mathcal{M} and the solution has been verified through the matching, one can positively determine whether M is homeomorphic to any other given hyperbolic manifold. However, if Orb fails to construct the structure, one has to prove by some other method that M is actually nonhyperbolic. This is what we do in the next section. In particular, we prove that the $113 - [(14 + 8 + 4) + 37] = 50$ elements of \mathcal{M}_{Σ_2} not covered by Propositions 3.3 and 3.4 are indeed nonhyperbolic, which implies the following:

Proposition 3.5. *The set $\mathcal{O}_{\Sigma_2}^{\text{hyp}}$ consists of the 63 manifolds described in Propositions 3.3 and 3.4.*

The elements of $\mathcal{O}_{\Sigma_2}^{\text{hyp}}$, together with the usual information on them determined by Orb, are listed in order of increasing volume in Table 4. Again the first column indicates the file from [Frigerio et al. 04b] where the manifold can be located in the position (starting from 0) specified in the second column. Note that the name of the file contains a description of the Kojima canonical decomposition (e.g., `tetra6` means that this decomposition consists of six tetrahedra).

3.4 Cusped Manifolds

We carried out the analysis of the hyperbolic elements of \mathcal{M}_{Σ_1} and $\mathcal{M}_{\Sigma_1 \sqcup \Sigma_1}$ using Orb, with the following result:

Proposition 3.6.

- The set \mathcal{M}_{Σ_1} (which has 81 elements) contains 11 hyperbolic manifolds, yielding 9 distinct homeomorphism types.
- The set $\mathcal{M}_{\Sigma_1 \sqcup \Sigma_1}$ (which has 9 elements) contains 2 distinct hyperbolic manifolds.

As above for the case of boundary Σ_2 , failure of Orb to find a cusped hyperbolic structure does not imply that the structure does not exist. However, in the next section we show that the $81 - 11 = 70$ elements of \mathcal{M}_{Σ_1} and the $9 - 2 = 7$ elements of $\mathcal{M}_{\Sigma_1 \sqcup \Sigma_1}$ not covered by Proposition 3.6 are indeed nonhyperbolic, which implies the following:

File	No.	Volume	Sym	Hom
census_3.snp	86	7.636519630	trivial	\mathbb{Z}^2
census_3.snp	87	7.636519630	\mathbb{Z}_2	\mathbb{Z}^2
census_3.snp	88	7.636519630	\mathbb{Z}_2	\mathbb{Z}^2
census_3.snp	89	7.636519630	\mathbb{Z}_2	\mathbb{Z}^2
census_3.snp	90	7.636519630	\mathbb{Z}_2	\mathbb{Z}^2
census_3.snp	91	7.636519630	\mathbb{Z}_2	\mathbb{Z}^2
census_3.snp	92	7.636519630	trivial	\mathbb{Z}^2
census_3.snp	93	7.636519630	\mathbb{Z}_2	\mathbb{Z}^2
census_3.snp	94	7.636519630	\mathbb{Z}_2	\mathbb{Z}^2
census_4_T2_tetra6.snp	0	8.297977385	\mathbb{Z}_2	\mathbb{Z}^2
census_4_T2_tetra6.snp	1	8.297977385	\mathbb{Z}_2	\mathbb{Z}^2
census_4_T2_tetra6.snp	2	8.297977385	\mathbb{Z}_2	\mathbb{Z}^2
census_4_T2_tetra4.snp	75	8.625848296	\mathbb{Z}_2	\mathbb{Z}^2
census_4_T2_tetra4.snp	76	8.625848296	\mathbb{Z}_2	\mathbb{Z}^2
census_4_T2_octa_nonreg.snp	0	8.739252140	D_3	$\mathbb{Z}_3 + \mathbb{Z}^2$
census_4_T2_octa_nonreg.snp	1	8.739252140	D_3	$\mathbb{Z}_3 + \mathbb{Z}^2$
census_4_T2_octa_nonreg.snp	2	8.739252140	\mathbb{Z}_2	\mathbb{Z}^2
census_4_T2_octa_nonreg.snp	3	8.739252140	\mathbb{Z}_2	\mathbb{Z}^2
census_4_T2_octa_nonreg.snp	4	8.739252140	\mathbb{Z}_2	\mathbb{Z}^2
census_4_T2_octa_nonreg.snp	5	8.739252140	\mathbb{Z}_2	\mathbb{Z}^2
census_4_T2_octa_nonreg.snp	6	8.739252140	D_3	$\mathbb{Z}_3 + \mathbb{Z}^2$
census_4_T2_octa_nonreg.snp	7	8.739252140	D_3	$\mathbb{Z}_3 + \mathbb{Z}^2$
census_4_T2_pyramids.snp	0	9.044841574	\mathbb{Z}_2	\mathbb{Z}^2
census_4_T2_pyramids.snp	1	9.044841574	\mathbb{Z}_2	\mathbb{Z}^2
census_4_T2_pyramids.snp	2	9.044841574	\mathbb{Z}_2	\mathbb{Z}^2
census_4_T2_pyramids.snp	3	9.044841574	\mathbb{Z}_2	\mathbb{Z}^2
census_4_T2_tetra4.snp	161	9.082538547	trivial	\mathbb{Z}^2
census_4_T2_tetra4.snp	162	9.082538547	trivial	\mathbb{Z}^2
census_4_T2_tetra4.snp	163	9.087925790	\mathbb{Z}_2	$\mathbb{Z}_3 + \mathbb{Z}^2$
census_4_T2_tetra4.snp	164	9.087925790	\mathbb{Z}_2	$\mathbb{Z}_3 + \mathbb{Z}^2$
census_4_T2_tetra4.snp	165	9.087925790	\mathbb{Z}_2	\mathbb{Z}^2
census_4_T2_tetra4.snp	166	9.087925790	\mathbb{Z}_2	\mathbb{Z}^2
census_4_T2_tetra5.snp	3	9.134474458	\mathbb{Z}_2	$\mathbb{Z}_2 + \mathbb{Z}^2$
census_4_T2_tetra5.snp	4	9.134474458	D_4	\mathbb{Z}^3
census_4_T2_tetra5.snp	5	9.134474458	D_4	\mathbb{Z}^3
census_4_T2_tetra5.snp	6	9.134474458	D_2	$\mathbb{Z}_2 + \mathbb{Z}^2$
census_4_T2_tetra5.snp	7	9.134474458	\mathbb{Z}_2	$\mathbb{Z}_2 + \mathbb{Z}^2$
census_4_T2_tetra5.snp	8	9.134474458	D_2	$\mathbb{Z}_2 + \mathbb{Z}^2$
census_4_T2_tetra5.snp	15	9.333442928	\mathbb{Z}_2	\mathbb{Z}^2
census_4_T2_tetra5.snp	16	9.333442928	trivial	\mathbb{Z}^2
census_4_T2_tetra5.snp	17	9.333442928	trivial	\mathbb{Z}^2
census_4_T2_tetra5.snp	18	9.333442928	\mathbb{Z}_2	\mathbb{Z}^2
census_4_T2_tetra5.snp	19	9.333442928	\mathbb{Z}_2	$\mathbb{Z}_3 + \mathbb{Z}^2$
census_4_T2_tetra5.snp	20	9.333442928	\mathbb{Z}_2	$\mathbb{Z}_3 + \mathbb{Z}^2$
census_4_T2_tetra4.snp	245	9.346204962	\mathbb{Z}_2	$\mathbb{Z}_3 + \mathbb{Z}^2$
census_4_T2_tetra4.snp	246	9.346204962	trivial	\mathbb{Z}^2
census_4_T2_tetra4.snp	247	9.346204962	\mathbb{Z}_2	\mathbb{Z}^2
census_4_T2_tetra5.snp	21	9.350261353	\mathbb{Z}_2	$\mathbb{Z}_3 + \mathbb{Z}^2$
census_4_T2_tetra5.snp	22	9.350261353	\mathbb{Z}_2	\mathbb{Z}^2
census_4_T2_octa_reg.snp	0	9.415841683	D_2	$\mathbb{Z}_3 + \mathbb{Z}^2$
census_4_T2_octa_reg.snp	1	9.415841683	D_4	$\mathbb{Z}/3 + \mathbb{Z}^2$
census_4_T2_octa_reg.snp	2	9.415841683	D_2	\mathbb{Z}^2
census_4_T2_octa_reg.snp	3	9.415841683	trivial	$\mathbb{Z}_2 + \mathbb{Z}^2$
census_4_T2_octa_reg.snp	4	9.415841683	\mathbb{Z}_2	$\mathbb{Z}_2 + \mathbb{Z}^2$
census_4_T2_octa_reg.snp	5	9.415841683	\mathbb{Z}_2	$\mathbb{Z}/2 + \mathbb{Z}^2$
census_4_T2_octa_reg.snp	6	9.415841683	D_3	$\mathbb{Z}_6 + \mathbb{Z}^2$
census_4_T2_octa_reg.snp	7	9.415841683	D_3	$\mathbb{Z}_6 + \mathbb{Z}^2$
census_4_T2_octa_reg.snp	8	9.415841683	trivial	$\mathbb{Z}_2 + \mathbb{Z}^2$
census_4_T2_octa_reg.snp	9	9.415841683	$\mathbb{Z}_2 + \mathbb{Z}_4$	$\mathbb{Z}_5 + \mathbb{Z}^2$
census_4_T2_octa_reg.snp	10	9.415841683	D_4	\mathbb{Z}^2
census_4_T2_octa_reg.snp	11	9.415841683	D_2	\mathbb{Z}^2
census_4_T2_octa_reg.snp	12	9.415841683	\mathbb{Z}_4	\mathbb{Z}^2
census_4_T2_octa_reg.snp	13	9.415841683	trivial	\mathbb{Z}^2

TABLE 4. Information on the 63 elements of $\mathcal{O}_{\Sigma_2}^{\text{hyp}}$ (the compact orientable hyperbolic manifolds with geodesic boundary of genus 2 arising from gluings of the octahedron).

Name	Volume	Sym	Hom
m006	2.568970601	D_2	$\mathbb{Z}_5 + \mathbb{Z}$
m007	2.568970601	D_2	$\mathbb{Z}_3 + \mathbb{Z}$
m009	2.666744783	D_2	$\mathbb{Z}_2 + \mathbb{Z}$
m010	2.666744783	D_2	$\mathbb{Z}_6 + \mathbb{Z}$
m011	2.781833912	\mathbb{Z}	\mathbb{Z}_2
m032	3.163963229	D_2	\mathbb{Z}
m033	3.163963229	D_2	$\mathbb{Z}_9 + \mathbb{Z}$
m036	3.177293279	D_2	$\mathbb{Z}_3 + \mathbb{Z}$
m038	3.177293279	D_2	\mathbb{Z}

TABLE 5. Information on the nine elements of $\mathcal{O}_{\Sigma_1}^{\text{hyp}}$ (the one-cusped orientable hyperbolic manifolds arising from gluings of the octahedron).

Name	Volume	Sym	Hom
m125	3.663862377	D_4	\mathbb{Z}^2
m129	3.663862377	D_4	\mathbb{Z}^2

TABLE 6. Information on the two elements of $\mathcal{O}_{\Sigma_1 \sqcup \Sigma_1}^{\text{hyp}}$ (the two-cusped orientable hyperbolic manifolds arising from gluings of the octahedron).

Proposition 3.7. *The set $\mathcal{O}_{\Sigma_1}^{\text{hyp}}$ (respectively, $\mathcal{O}_{\Sigma_1 \sqcup \Sigma_1}^{\text{hyp}}$) consists of the nine (respectively, two) manifolds described in Proposition 3.6.*

Using Orb we have determined the symmetry group and homology of each element of $\mathcal{O}_{\Sigma_1}^{\text{hyp}}$ and $\mathcal{O}_{\Sigma_1 \sqcup \Sigma_1}^{\text{hyp}}$, together with the name it was given in [Callahan et al. 99, Weeks 93]. This information appears in Tables 5 and 6.

4. NONHYPERBOLIC MANIFOLDS

In this section we analyze the elements of \mathcal{M} not covered by Propositions 3.1, 3.2, 3.3, 3.4, and 3.6, thus completing our enumeration of \mathcal{O} . Recall that only \mathcal{M}_{\emptyset} , \mathcal{M}_{Σ_1} , $\mathcal{M}_{\Sigma_1 \sqcup \Sigma_1}$, and \mathcal{M}_{Σ_2} still require some work.

4.1 Matching of Triangulations

The numbers of elements of \mathcal{M}_{Σ} not already recognized as belonging to $\mathcal{O}_{\Sigma}^{\text{hyp}}$ are as described in the central column of Table 7. As already remarked, all these manifolds come with a triangulation consisting of four tetrahedra. Now, one of the features of Orb is to compare two triangulated manifolds for equality by randomizing the initial triangulations and matching. So we have first exploited this feature to reduce the numbers of potentially distinct homeomorphism types, getting the results described in the rightmost column of Table 7. In the rest of this section we describe the proof of the following result:

Type According to the Boundary	Apparently Nonhyperbolic	Apparently Distinct After Matching
\mathcal{M}_{\emptyset}	37	17
\mathcal{M}_{Σ_1}	70	21
$\mathcal{M}_{\Sigma_1 \sqcup \Sigma_1}$	7	5
\mathcal{M}_{Σ_2}	50	16
$\mathcal{M}_{\Sigma_2 \sqcup \Sigma_1}$	–	–
\mathcal{M}_{Σ_3}	–	–

TABLE 7. Numbers of apparently nonhyperbolic elements of \mathcal{M} , and potentially distinct homeomorphism types after the triangulation matching performed using Orb.

Proposition 4.1. *For $\Sigma = \emptyset, \Sigma_1, \Sigma_1 \sqcup \Sigma_1, \Sigma_2$ and $I = 17, 21, 5, 16$, respectively, let $(M_{\Sigma}^{(i)})_{i=1}^I$ be the manifolds as in the rightmost column of Table 7. Then:*

1. *If $i \neq j$, then $M_{\Sigma}^{(i)}$ is not homeomorphic to $M_{\Sigma}^{(j)}$.*
2. *Each $M_{\Sigma}^{(i)}$ is nonhyperbolic.*

This implies Propositions 3.5 and 3.7, the equalities $\mathcal{O}_{\Sigma}^{\text{non}} = (M_{\Sigma}^{(i)})_{i=1}^I$ for all four relevant Σ 's, and hence Theorem 1.1. Our proof utilizes computers and theoretical work. Note that Proposition 4.1 shows that Orb was totally efficient both in constructing the hyperbolic structures and in comparing the nonhyperbolic manifolds for homeomorphism.

In the sequel we freely use several classical notions, results, and techniques of 3-manifold topology, in particular the definition of essential surface, the Haken–Kneser–Milnor decomposition along spheres, the definition and properties of Seifert fibered spaces, and the Jaco–Shalen–Johansson decomposition along tori and annuli; see [Hempel 76, Fomenko and Matveev 97, Matveev 03]. Moreover, we use the fact that if a manifold contains a properly embedded essential surface with nonnegative Euler characteristic, then the manifold cannot be hyperbolic.

4.2 The 3-Manifold Recognizer

As already mentioned, besides Orb we have employed another piece of software, namely the 3-Manifold Recognizer [Matveev and Tarkaev 06]. The input to this program is a triangulation of a 3-manifold M , and its output is the “name” of M , by which we mean the following:

- For a Seifert M , (one of) its Seifert structure(s).
- For a hyperbolic M , its presentation(s) as a Dehn filling of a manifold in the tables of Weeks [Callahan et al. 99].

- For an irreducible M having JSJ decomposition into more than one block, the names (as just illustrated) of the blocks, together with the gluing instructions between the blocks.
- For a reducible manifold, the names (as just illustrated) of its irreducible summands.

The program is not guaranteed always to find the name of the manifold (for instance, it does not even attempt to do this for manifolds with boundary of genus 2 or more, and it happens to fail also in other cases). But it can always compute the first homology and, in the case of boundary of genus at most 1, the Turaev–Viro invariants [Turaev and Viro 92], which turned out to be very useful for us.

We now describe the proof of Proposition 4.1, breaking it into separate sections according to the boundary type Σ , and at the same time we provide detailed topological information on the manifolds $M_\Sigma^{(i)}$.

4.2.1 Closed Manifolds. Let us start with the case $\Sigma = \emptyset$. The second item in Proposition 4.1, namely the proof that each $M_\emptyset^{(i)}$ is nonhyperbolic, was not an issue in this case. In fact, it has been known for a long time [Matveev 03] that any triangulation of a closed hyperbolic manifold contains at least nine tetrahedra, whereas each $M_\emptyset^{(i)}$ admits a triangulation with four tetrahedra.

To show that $M_\emptyset^{(i)} \not\cong M_\emptyset^{(j)}$ for $1 \leq i < j \leq 17$, we ran the Recognizer, which successfully identified all the manifolds (this was also independently done by Tarkaev). From the names (all manifolds turned out to be Seifert or connected sums of Seifert) we could see that the $M_\emptyset^{(i)}$'s were indeed all distinct, except possibly for $M_\emptyset^{(1)}$ and $M_\emptyset^{(2)}$, which were both recognized to be the connected sum of two copies of the lens space $L(3, 1)$. Since $L(3, 1)$ has no orientation-reversing automorphism, even if one looks (as we do) at orientable but unoriented manifolds, there are two distinct ways of performing the connected sum of $L(3, 1)$ with itself, so the names of $M_\emptyset^{(1)}$ and $M_\emptyset^{(2)}$ provided by the Recognizer were indeed ambiguous.

To show that $M_\emptyset^{(1)} \not\cong M_\emptyset^{(2)}$, we then had to examine their triangulations by hand, introducing an arbitrary orientation on each and finding the essential sphere realizing the connected sum. Cutting along this sphere and capping off, we saw that for $M_\emptyset^{(1)}$, the two connected summands were distinctly oriented copies of $L(3, 1)$, while for $M_\emptyset^{(2)}$, they were consistently oriented. This led us to the proof of Proposition 4.1 for $\Sigma = \emptyset$. More precisely, we established the following:

Proposition 4.2. *The set $\mathcal{O}_\emptyset^{\text{non}}$ consists of 13 irreducible manifolds and 4 reducible ones. The irreducible manifolds are the Seifert spaces*

$$\begin{aligned} & \mathbb{S}^3, \quad \mathbb{P}^3, \quad \mathbb{S}^2 \times \mathbb{S}^1, \quad L(3, 1), \quad L(4, 1), \quad L(5, 2), \\ & L(6, 1), \quad L(9, 2), \quad L(12, 5), \quad (\mathbb{P}^2; (3, 2), (1, 0)), \\ & (\mathbb{P}^2; (2, 1), (1, 1)), \quad (\mathbb{P}^2; (1, 3)), \\ & (\mathbb{S}^2; (2, 1), (3, 1), (3, 1), (1, -1)), \end{aligned}$$

and the reducible ones are

$$\begin{aligned} & \mathbb{P}^3 \# \mathbb{P}^3, \quad \mathbb{P}^3 \# L(3, 1), \quad L(3, 1) \# L(3, 1), \\ & L(3, 1) \# (-L(3, 1)). \end{aligned}$$

4.2.2 One-Cusped Manifolds. In this case, both items in Proposition 4.1 required some work. We proceeded as follows.

To prove that $M_{\Sigma_1}^{(i)} \not\cong M_{\Sigma_1}^{(j)}$ for $1 \leq i < j \leq 21$, we again employed the Recognizer, calculating the first homology group and Turaev–Viro invariants up to order 16 of each $M_{\Sigma_1}^{(i)}$. From this computation we deduced that $M_{\Sigma_1}^{(i)} \not\cong M_{\Sigma_1}^{(j)}$ for $1 \leq i < j \leq 21$ except possibly for $i = 1, 2, 3, 4$ and $j = i + 4$. For the remaining four pairs of manifolds, we showed that the homeomorphism was impossible by analyzing the JSJ decompositions. Specifically, $M_{\Sigma_1}^{(1)}$ and $M_{\Sigma_1}^{(5)}$ turned out to be Seifert and distinct, and the same happened for $M_{\Sigma_1}^{(2)}$ and $M_{\Sigma_1}^{(6)}$, whereas $M_{\Sigma_1}^{(3)}$ and $M_{\Sigma_1}^{(7)}$ had nontrivial JSJ decompositions, with the same blocks but different gluing matrices, and analogously for $M_{\Sigma_1}^{(4)}$ and $M_{\Sigma_1}^{(8)}$.

The results just described allowed us to conclude that $M_{\Sigma_1}^{(i)}$ is nonhyperbolic for $i = 1, \dots, 8$. To show that the same holds for $i = 9, \dots, 21$, we used the Recognizer again to compute connected-sum and JSJ decompositions. In each instance the desired result was returned because we obtained either connected sums or manifolds having JSJ decomposition consisting of Seifert pieces (sometimes only one of them). It is perhaps worth mentioning that in one case the Recognizer failed to return the answer right away, but we were able to transform the triangulation by hand into one that the Recognizer could handle.

These arguments led us to the proof of Proposition 4.1 for the case $\Sigma = \Sigma_1$, and also to the next, more specific, result. In its statement we use matrices to encode gluings between boundary components of Seifert spaces, which requires choosing homology bases; when the base surface of the fibration is orientable, the homology basis is (μ, λ) , where μ is a boundary component of the base surface of

the fibration and λ is a fiber; see [Fomenko and Matveev 97] for the nonorientable case.

Proposition 4.3. *The 21 elements of the set $\mathcal{O}_{\Sigma_1}^{\text{non}}$ subdivide as follows:*

- two reducible manifolds, both being the connected sum of two Seifert spaces;
- ten irreducible Seifert spaces;
- seven irreducible manifolds whose JSJ decomposition consists of two Seifert blocks;
- two irreducible manifolds whose JSJ decomposition consists of three Seifert blocks.

More precisely:

- The two reducible manifolds are $\mathbb{P}^3 \# (D^2 \times \mathbb{S}^1)$ and $L(3, 1) \# (D^2 \times \mathbb{S}^1)$.

- The ten Seifert spaces are

$$D^2 \times \mathbb{S}^1, (\mathbb{S}^2 \setminus 3D^2, (1, 0)),$$

$$(D^2, (2, 1), (2, 1), (1, 0)), (D^2, (2, 1), (3, 1), (1, -1)),$$

$$(D^2, (3, 1), (3, 2), (1, 0)), (D^2, (3, 2), (3, 2), (1, -1)),$$

$$(D^2, (3, 2), (4, 1), (1, -1)), (D^2, (3, 1), (4, 1), (1, 0)),$$

$$(\mathbb{P}^2 \setminus D^2, (2, 1), (1, 0)), (\mathbb{P}^2 \setminus D^2, (3, 2), (1, 0)).$$

- The seven manifolds having JSJ decomposition consisting of two Seifert blocks are obtained by gluing the following pairs of Seifert spaces along the homeomorphism represented by the matrix $\begin{pmatrix} 0 & 1 \\ 1 & 0 \end{pmatrix}$:

$$(\mathbb{S}^2 \setminus 2D^2, (2, 1), (1, 0)), (D^2, (2, 1), (2, 1), (1, 0));$$

$$(\mathbb{S}^2 \setminus 2D^2, (2, 1), (1, 1)), (D^2, (2, 1), (4, 3), (1, -1));$$

$$(\mathbb{S}^2 \setminus 2D^2, (3, 1), (1, -1)), (D^2, (2, 1), (3, 2), (1, -1));$$

$$(\mathbb{S}^2 \setminus 2D^2, (3, 2), (1, 0)), (D^2, (2, 1), (3, 2), (1, -1));$$

$$(\mathbb{S}^2 \setminus 2D^2, (2, 1), (1, 0)), (D^2, (3, 1), (3, 2), (1, -1));$$

$$(\mathbb{S}^2 \setminus 2D^2, (2, 1), (1, -1)), (D^2, (3, 1), (3, 1), (1, -1));$$

$$(\mathbb{P}^2 \setminus 2D^2, (1, 1)) (D^2, (2, 1), (3, 1), (1, -1)).$$

- The two manifolds having JSJ decomposition consisting of three Seifert blocks are obtained by gluing two Seifert spaces to two different boundary components of $(\mathbb{S}^2 \setminus 3D^2, (1, 2))$. In the first example the remaining two Seifert blocks are both $(D^2, (2, 1), (3, 2), (1, -1))$. In the second example the remaining two Seifert blocks are $(D^2, (2, 1), (3, 1), (1, -1))$ and $(D^2, (2, 1), (3, 2), (1, -1))$. The gluing homeomorphisms are all encoded by the matrix $\begin{pmatrix} 0 & 1 \\ 1 & 0 \end{pmatrix}$.

Remark 4.4. The fact that $M_{\Sigma_1}^{(3)}$ and $M_{\Sigma_1}^{(7)}$ have JSJ decompositions with the same two blocks but different gluing matrices, and analogously for $M_{\Sigma_1}^{(4)}$ and $M_{\Sigma_1}^{(8)}$, can be recovered from the statement just given by changing some parameters of the exceptional fiber. This allows one to get identical presentations of some Seifert spaces but different gluing matrices.

4.2.3 Two-Cusped Manifolds. For the case $\Sigma = \Sigma_1 \sqcup \Sigma_1$ we had to deal with five manifolds, which we did using the Recognizer. To show that they are distinct we computed their Turaev–Viro invariants, which led to the desired conclusion right away. To prove that they are not hyperbolic we determined their JSJ decomposition, which always turned out to consist of Seifert blocks, whence the conclusion. More precisely we established the following:

Proposition 4.5. *All five elements of $\mathcal{O}_{\Sigma_1 \sqcup \Sigma_1}^{\text{non}}$ are irreducible. Three of them are Seifert spaces and two have JSJ decomposition consisting of two Seifert blocks. The Seifert spaces are*

$$\Sigma_1 \times [0, 1], (\mathbb{S}^2 \setminus 2D^2; (2, 1), (1, -1)),$$

$$(\mathbb{S}^2 \setminus 2D^2; (3, 2), (1, 1));$$

the Seifert blocks for the two other manifolds are respectively $(\mathbb{S}^2 \setminus 3D^2; (1, 0))$ and $(D^2; (2, 1), (3, 1), (1, -1))$, and two copies of $(\mathbb{S}^2 \setminus 2D^2; (2, 1), (1, -1))$, while the gluing is encoded by the matrix $\begin{pmatrix} 0 & 1 \\ 1 & 0 \end{pmatrix}$ in both cases.

4.2.4 Genus-2 Boundary: Distinguishing Manifolds. The case of genus-2 boundary was the hardest to settle, in particular because it could not be dealt with using the Recognizer. We concentrate here on the task of showing that $M_{\Sigma_2}^{(i)} \not\cong M_{\Sigma_2}^{(j)}$ for $1 \leq i < j \leq 16$ (item 1 of Proposition 4.1), postponing the proof of nonhyperbolicity to another section. We proceeded as follows:

1. We first analyzed (by hand) the Turaev–Viro invariants of each $M_{\Sigma_2}^{(i)}$. This allowed us to break down our set of 16 manifolds into three groups of four manifolds, one group of two, and two groups of one, such that the manifolds in each group have the same Turaev–Viro invariants of all orders, while manifolds in different groups have a distinct Turaev–Viro invariant (of order 6 or 7, as it turned out).
2. Then we determined (by computer) the homology of the threefold coverings of the manifolds in each group. This allowed us to conclude that $M_{\Sigma_2}^{(i)} \not\cong$

$M_{\Sigma_2}^{(j)}$ for $1 \leq i < j \leq 16$ except possibly $i = 1, 3$ and $j = i + 1$. Moreover, it was not difficult to show that $\pi_1(M_{\Sigma_2}^{(i)}) = \pi_1(M_{\Sigma_2}^{(i+1)})$ for $i = 1, 3$ (and in fact previously we had also shown that $M_{\Sigma_2}^{(i)}$ and $M_{\Sigma_2}^{(i+1)}$ have the same Turaev–Viro invariants of all orders).

3. To deal with the remaining two pairs $M_{\Sigma_2}^{(1)}, M_{\Sigma_2}^{(2)}$ and $M_{\Sigma_2}^{(3)}, M_{\Sigma_2}^{(4)}$, the strategy was to find their JSJ decompositions. Below we explain in some detail how this was done.

The general idea was to switch from triangulations to the dual viewpoint of special spines of 3-manifolds, and more generally to *simple* spines [Matveev 03]. The reason why this was beneficial in this case is that a special spine that contains a 2-component with embedded closure incident to two vertices (as our spines turned out to do) admits a so-called inverse L-move [Matveev 03], whose result is a simple spine of the same manifold. In particular, this spine may contain an annulus (or Möbius-strip) 2-component, and it frequently turns out that the annulus transversal to the core of the annulus 2-component (or to the boundary of the Möbius strip) is essential. Moreover, if the initial spine has a small number of vertices, one may hope that after cutting along the annulus, the spine breaks down into easily identifiable pieces (for instance, polyhedra that collapse onto graphs), in which case the annulus already constitutes the JSJ splitting surface of the manifold in question. This is precisely the strategy that worked in our case.

Let us now turn to our specific situation. After dualizing the triangulations and applying the inverse L-move, we obtained the simple spines P_1, \dots, P_4 shown in Figure 1.

As explained in the caption, the spines of $M_{\Sigma_2}^{(1)}$ and $M_{\Sigma_2}^{(2)}$ contain an annular 2-component, while those of $M_{\Sigma_2}^{(3)}$ and $M_{\Sigma_2}^{(4)}$ contain a Möbius-strip 2-component. Let us denote by S_i the properly embedded annulus or Möbius strip transversal to the curve α_i also described in the caption of Figure 1.

We begin with the case $i = 1, 2$. As one sees from the picture, cutting P_i along α_i , one gets a disjoint union of two polyhedra that collapse respectively onto a circle and onto a graph of Euler characteristic -1 . Since this corresponds to cutting $M_{\Sigma_2}^{(i)}$ along S_i , we deduce that $M_{\Sigma_2}^{(i)}$ is obtained by gluing a genus-2 handlebody and a solid torus along a boundary annulus. Looking at the core curves of the glued annuli, it is not difficult to show that the annulus S_i is essential in $M_{\Sigma_2}^{(i)}$, so it gives the JSJ decomposition. Finally, making a closer examination

of the gluings, we saw that the annuli used in both gluings are the same, while the gluing homeomorphisms are different. This allowed us to conclude that $M_{\Sigma_2}^{(1)} \not\cong M_{\Sigma_2}^{(2)}$.

Let us now turn to the case $i = 3, 4$. Cutting P_i along the core circle of the Möbius-strip component (which again corresponds to cutting $M_{\Sigma_2}^{(i)}$ along S_i) yields a polyhedron that collapses onto a graph of Euler characteristic -1 . Even if we get a single polyhedron (which must be the case, since this time the cut is along the core of a Möbius strip), we again conclude that the initial manifold is obtained by gluing a genus-2 handlebody and a solid torus along a boundary annulus. As before, it is not hard to show that the annulus is in fact essential, so it gives the JSJ decomposition. In addition, we have proved that the annulus in the boundary of the solid torus is the same in both cases, its core being the curve of type $(2, 1)$. In contrast, the cores of the annuli on the boundary of the genus-2 handlebody used to obtain $M_{\Sigma_2}^{(3)}$ and $M_{\Sigma_2}^{(4)}$ are those shown in Figure 2.

The conclusion that $M_{\Sigma_2}^{(3)} \not\cong M_{\Sigma_2}^{(4)}$ now follows from the next result, the long proof of which we only outline:

Proposition 4.6. *No homeomorphism of the genus-2 handlebody H takes the curve ℓ_3 shown in Figure 2 (left) to the curve ℓ_4 shown in Figure 2 (right).*

Proof: As already mentioned, we restrict ourselves to indicating the general scheme of our argument only. As one sees from Figure 2, for $i = 3, 4$ there exists an essential disk D_i in H that intersects ℓ_i transversely in exactly two points. Moreover, cutting H along D_i , we get two solid tori T_i^0 and T_i^1 such that ∂T_i^j contains a distinguished disk Δ_i^j and an arc β_i^j properly embedded in $\partial T_i^j \setminus \Delta_i^j$. The pair (H, ℓ_i) is obtained by gluing T_i^0 to T_i^1 along a homeomorphism $\Delta_i^0 \rightarrow \Delta_i^1$, with ℓ_i being the image of $\beta_i^0 \cup \beta_i^1$. It is actually quite easy to see that the four triples $(T_i^j, \Delta_i^j, \beta_i^j)$ for $i = 3, 4$ and $j = 0, 1$ can be identified with each other, but after doing this, the gluing homeomorphisms $\Delta_3^0 \rightarrow \Delta_3^1$ and $\Delta_4^0 \rightarrow \Delta_4^1$ differ by a rotation of angle π , which is isotopic to the identity but not in a way that preserves the endpoints of the arcs. The proof of the proposition then follows from this claim:

Claim 4.7. *For $\ell \in \{\ell_3, \ell_4\}$, the disk D properly embedded in H that intersects ℓ transversely in two points and splits H into two solid tori is unique up to isotopy preserving ℓ .*

The proof of this claim is rather long and technical. We consider a handle decomposition of H into one 0-handle and two 1-handles. This yields a decomposition

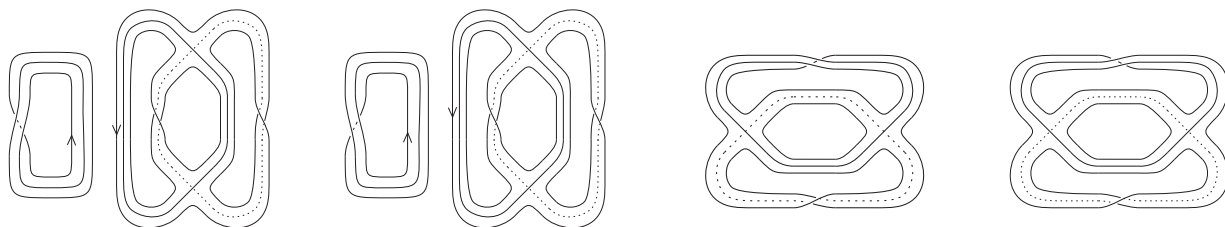


FIGURE 1. The simple spines P_1, \dots, P_4 of $M_{\Sigma_2}^{(1)}, \dots, M_{\Sigma_2}^{(4)}$. The picture always shows the boundary of a regular neighborhood of the locus of nonsurface points. To get P_1 from the two separate fragments shown, one must identify the two curves marked by arrows, which constitute the core α_1 of the annular 2-component of P_1 , while all other 2-components are disks. The same applies to P_2 , which contains an annulus with core α_2 . To get P_3 from the fragment shown, one should attach a Möbius strip to the “long” curve α_3 and a disk to the other one, and the same applies to P_4 , which contains a Möbius strip bounded by a curve α_4 .

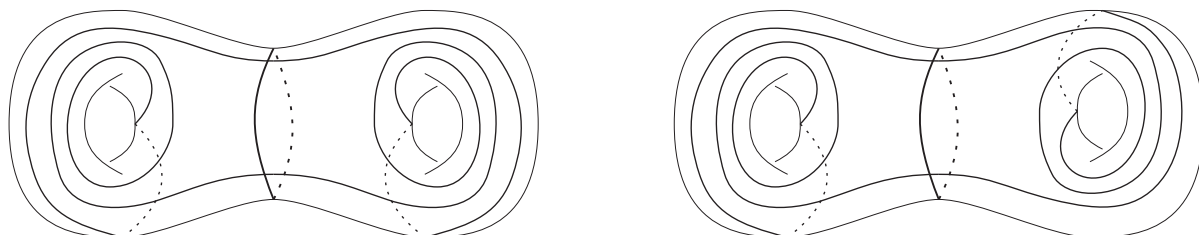


FIGURE 2. The core curves of the annuli used to reconstruct $M_{\Sigma_2}^{(3)}$ and $M_{\Sigma_2}^{(4)}$.

of ∂H into three punctured disks: one sphere with four holes, and two annuli. Slightly modifying the definition in [Matveev 03], we then call *normal* with respect to this decomposition a curve in ∂H that intersects each of the punctured disks along a collection of simple arcs with endpoints on different boundary components or along a simple closed curve. We next establish the following two facts:

1. Up to isotopy preserving ℓ , there is a unique normal curve that intersects ℓ in two points and decomposes H into two solid tori.
2. The boundary of D can be isotoped (preserving ℓ) to normal position.

This concludes our argument. □

4.2.5 Genus-2 Boundary: Nonhyperbolicity. To show that none of the manifolds $M_{\Sigma_2}^{(i)}$ is hyperbolic, we used again the idea described above. Namely, we constructed for each $M_{\Sigma_2}^{(i)}$ a simple spine with an annulus or Möbius-strip component, and we proved that the corresponding proper annulus in the manifold is essential. This was done as follows:

1. For about half of the $M_{\Sigma_2}^{(i)}$'s, the special spine dual to the initial triangulation already contained a 2-component incident to two vertices, so we found

a simple spine with an annulus or Möbius-strip 2-component by applying an inverse L-move, as above. For the other $M_{\Sigma_2}^{(i)}$'s we did the same, but we first had to change the initial special spine, by applying first one positive T-move [Matveev 03] and then one inverse T-move elsewhere.

2. From the spine of $M_{\Sigma_2}^{(i)}$ constructed in the previous item we obtained a properly embedded annulus S_i , which we then showed to be essential. We did this by cutting $M_{\Sigma_2}^{(i)}$ along S_i , which gave the following:
 - (a) In two cases, a genus-2 handlebody.
 - (b) In six cases, the union of a genus-2 handlebody and a solid torus.
 - (c) In four cases, a manifold that could be further split along an annulus into the union of a genus-2 handlebody and a solid torus.
 - (d) In four cases, the union of a solid torus and a manifold as described in the previous point.

In all cases, analyzing the way $M_{\Sigma_2}^{(i)}$ can be reconstructed from the pieces S_i cuts it into, we could then show that it is irreducible and that within it S_i is π_1 -injective and not boundary-parallel, from which we obtained the desired conclusion.

4.2.6 Further Information for Genus-2 Boundary. The decomposition (a)–(d) just described along annuli of the 16 elements of $\mathcal{O}_{\Sigma_2}^{\text{non}}$ provides a rather accurate description of the topology of these manifolds. In addition to it, we mention that in cases (c) and (d), the second splitting annulus is not disjoint from the trace of S_i , so the splitting cannot be described as being along the union of two disjoint annuli.

ACKNOWLEDGMENTS

Part of this work was carried out while the third-named author was visiting the University of Melbourne, Université Paul Sabatier in Toulouse, and Columbia University in New York. He is grateful to all these institutions for financial support, and he would like to thank Craig Hodgson, Michel Boileau, and Dylan Thurston for their warm hospitality and inspiring mathematical discussions. The second-named author was supported by the Marie Curie fellowship MIF1-CT-2006-038734.

REFERENCES

- [Benedetti and Petronio 92] R. Benedetti and C. Petronio. *Lectures on Hyperbolic Geometry*. New York: Springer-Verlag, 1992.
- [Callahan et al. 99] P. J. Callahan, M. V. Hildebrandt, and J. R. Weeks. “A Census of Cusped Hyperbolic 3-Manifolds,” with microfiche supplement. *Math. Comp.* 68 (1999), 321–332.
- [Coulson et al. 00] D. Coulson, O. Goodman, C. Hodgson, and W. Neumann. “Computing Arithmetic Invariants of 3-Manifolds.” *Experiment. Math.* 9 (2000), 127–152.
- [Epstein and Penner 88] D. B. A. Epstein and R. C. Penner. “Euclidean Decomposition of Non-compact Hyperbolic Manifolds.” *J. Differential Geom.* (1) 27 (1988), 67–80.
- [Fomenko and Matveev 97] A. T. Fomenko and S. V. Matveev. *Algorithmic and Computer Methods for Three-Manifolds*, Mathematics and Its Applications 425. Dordrecht: Kluwer Academic Publishers, 1997.
- [Frigerio and Petronio 04] R. Frigerio and C. Petronio. “Construction and Recognition of Hyperbolic 3-Manifolds with Geodesic Boundary.” *Trans. Amer. Math. Soc.* 356 (2004), 3243–3282.
- [Frigerio et al. 04a] R. Frigerio, B. Martelli, and C. Petronio. “Small Hyperbolic 3-Manifolds with Geodesic Bboundary.” *Experiment. Math.* 13 (2004), 171–184.
- [Frigerio et al. 04b] R. Frigerio, B. Martelli, and C. Petronio. “Hyperbolic 3-Manifolds with Non-empty Boundary.” Tables available online (www.dm.unipi.it/pages/petronio/public_html), 2004.
- [Goodman 03] O. Goodman. “Snap,” A Computer Program for Studying Arithmetic Invariants of Hyperbolic 3-Manifolds. Available online (<http://www.ms.unimelb.edu.au/~snap/> and <http://sourceforge.net/projects/snap-pari>), 2003.
- [Haken 61] W. Haken. “Theorie der Normalflächen: Ein Isotopiekriterium für den Kreisknoten.” *Acta Math.* 105 (1961), 245–375.
- [Heard 06] D. Heard. “Orb,” A Computer Program for Finding Hyperbolic Structures on Hyperbolic 3-Orbifolds and 3-Manifolds. Available online (<http://www.ms.unimelb.edu.au/~snap/orb.html>), 2006.
- [Heard et al. 08] Damian Heard, Ekaterina Pervova, and Carlo Petronio. “Census of the 191 Orientable Octahedral Manifolds.” Available online (http://www.dm.unipi.it/pages/petronio/public_html/octa.html), 2008.
- [Hempel 76] J. Hempel. *3-Manifolds*, Ann. of Math. Studies 86. Princeton: Princeton University Press, 1976.
- [Jaco and Shalen 78] W. Jaco and P. B. Shalen. “A New Decomposition Theorem for Irreducible Sufficiently-Large 3-Manifolds.” *Algebraic and Geometric Topology (Proc. Sympos. Pure Math., Stanford Univ., Stanford, Calif., 1976)*, part 2, pp. 71–84, Proc. Sympos. Pure Math. XXXII. Providence: Amer. Math. Soc., 1978.
- [Johannson 79] K. Johannson. *Homotopy Equivalences of 3-Manifolds with Boundaries*, Lecture Notes in Mathematics 761. Berlin: Springer-Verlag, 1979.
- [Kojima 90] S. Kojima. “Polyhedral Decomposition of Hyperbolic Manifolds with Boundary.” *Proc. Work. Pure Math.* 10 (1990), 37–57.
- [Kojima 92] S. Kojima. “Polyhedral Decomposition of Hyperbolic 3-Manifolds with Totally Geodesic Boundary.” In *Aspects of Low-Dimensional Manifolds*, pp. 93–112, Adv. Stud. Pure Math. 20. Tokyo: Kinokuniya, 1992.
- [Matveev 03] S. V. Matveev. *Algorithmic Topology and Classification of 3-Manifolds*, ACM Monographs 9. New York: Springer, 2003.
- [Matveev and Tarkaev 06] S. V. Matveev and V. V. Tarkaev, “Three-manifold Recognizer,” A Computer Program for Recognition of 3-Manifolds. Available online (<http://www.csu.ac.ru/~trk/spine/>), 2006.
- [Perelman 02] G. Perelman. “The Entropy Formula for the Ricci Flow and Its Geometric Applications.” Preprint; math.DG/0211159, 2002.
- [Perelman 03a] G. Perelman. “Ricci Flow with Surgery on Three-Manifolds.” Preprint; math.DG/0303109, 2003.
- [Perelman 03b] G. Perelman. “Finite Extinction Time for the Solutions to the Ricci Flow on Certain Three-Manifolds.” Preprint; math.DG/0307245, 2003.
- [Ratcliffe 06] J. G. Ratcliffe. *Foundations of Hyperbolic Manifolds*, 2nd edition, Graduate Texts in Math. 149. New York: Springer, 2006.

- [Rourke and Sanderson 72] C. P. Rourke and B. J. Sanderson. *Introduction to Piecewise-Linear Topology*, *Ergebn. der Math.* 69. New York: Springer-Verlag, 1972.
- [Sakuma and Weeks 95] M. Sakuma and J. R. Weeks. “The Generalized Tilt Formula.” *Geom. Dedicata* 50 (1995), 1–9.
- [Thurston 79] W. P. Thurston. “The Geometry and Topology of 3-manifolds.” Mimeographed notes, Princeton, 1979.
- [Turaev and Viro 92] V. G. Turaev and O. Ya. Viro. “State Sum Invariants of 3-Manifolds and Quantum $6j$ -Symbols.” *Topology (4)* 31 (1992), 865–902.
- [Ushijima 02] A. Ushijima. “The Tilt Formula for Generalized Simplices in Hyperbolic Space.” *Discrete Comput. Geom.* 28 (2002), 19–27.
- [Ushijima 06] A. Ushijima. “A Volume Formula for Generalised Hyperbolic Tetrahedra.” In *Non-Euclidean Geometries*, pp. 249–265, *Mathematics and Its Applications* 581. New York: Springer, 2006.
- [Weeks 93] J. R. Weeks. “SnapPea,” The Hyperbolic Structures Computer Program. Available online (<http://www.geometrygames.org>), 1993.

Damian Heard, RedTribe, Carlton, Victoria, Australia 3053 (damianh@redtribe.com)

Ekaterina Pervova, Dipartimento di Matematica Applicata, Via Filippo Buonarroti, 1C, 56127 Pisa, Italy
(pervova@guest.dma.unipi.it)

Carlo Petronio, Dipartimento di Matematica Applicata, Via Filippo Buonarroti, 1C, 56127 Pisa, Italy (petronio@dm.unipi.it)

Received September 13, 2007; accepted in revised form June 11, 2008.